ChemComm

Accepted Manuscript

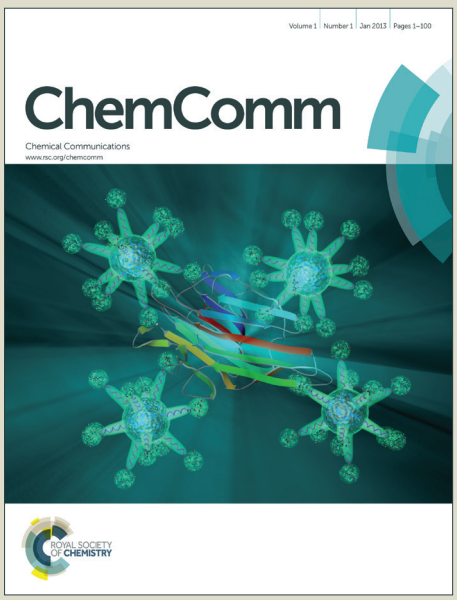

ROYAL SOCIETY OF CHEMISTRY

www.rsc.org/chemcomm

ChemComm

COMMUNICATION

Received 00th January 20xx,

GdDOTAGA(C_{18})$_2$: an efficient amphiphilic Gd(III) chelate for the preparation of self-assembled high relaxivity MRI nanoprobes ‡

M. Filippi,[a] D. Remotti,[b] M. Botta,[b] E. Terreno,[a] and L. Tei[b*]

Accepted 00th January 20xx

DOI: 10.1039/x0xx00000x

www.rsc.org/

A new amphiphilic GdDOTA-like complex functionalized with two octadecyl chains was synthesised and incorporated into the bilayer of liposomes and dendrimersomes. ^{1}H NMR relaxometric studies and *in vivo* MRI experiments on mice bearing a syngeneic melanoma tumour have shown a great improvement in performance.

In the last few years, nanomedicine has tremendously grown due to the great progresses achieved in the fields of nanotechnology, pharmacology, and molecular imaging.[1,2] The versatility of nanosystems allows tuneable surface modification and loading with different chemicals (drugs, imaging agents, targeting vectors) with the aim of fine-optimizing the biological properties of the nanocarriers, while simultaneously enabling them to perform diagnostically and/or therapeutically important functions.[3,4]
Lipid-containing nanoparticles (LNPs),[5] like micelles, liposomes, and solid lipid nanoparticles, or other similar nanosystems (such as the recently developed dendrimersomes)[6-8] are based on supramolecular aggregates obtained by spontaneous assembling in aqueous solution of phospholipids alone or in mixture with other amphiphilic molecules. Such objects have been frequently used as nanocarriers for drug delivery and imaging applications due to their great chemical versatility that allows the loading of hydrophobic, amphiphilic, and hydrophilic substances, and surface decoration with targeting vectors, blood lifetime modulators, and diagnostic agents.[7-9] Moreover, several liposomal drug formulations have already been clinically approved for cancer treatment thanks to their ability to passively accumulate in the tumour tissue.[10,11]
As far as theranostics is concerned, the use of nanoparticles can be also favourable for increasing the detection threshold of the imaging agent.[12] This is particularly relevant for MRI, where the relatively low sensitivity of the technique can be overcome by delivering a high number of paramagnetic Gd(III) complexes at the biological target.[13] Furthermore, the incorporation of an amphiphilic agent in the particle membrane can substantially improve its longitudinal relaxivity r_1 (in the magnetic field range 0.5 – 3 T) due to the restriction of the tumbling motion of the agent.[14,15] So far, the most used amphiphilic Gd-agents have been: i) Gd-DTPA-bisamide derivatives bearing long aliphatic chains (e.g. Gd-DTPA-BSA)[16,17], ii) a Gd-DOTA monoamide conjugated to two octadecyl tails (GdDOTAMA(C_{18})$_2$),[16,18] and iii) a Gd-DOTA-monoamide conjugated to the polar head of a phospholipid (1,2-distearoyl-sn-glycero-3-phospho ethanolamine, DSPE) through a short C2 spacer.[19] With respect to DTPA-bisamides, the two macrocyclic systems offer the advantage of much higher thermodynamic and kinetic stabilities, as well as higher relaxivities. The proton relaxivity of a discrete incorporated complex is often quite modest, typically 10–20 mM^{-1}s^{-1} (25 °C, 0.5 T), much less than the highest values predicted by theory. The two major limiting factors are the slow water exchange rate ($k_{ex} = 1/\tau_M$) of the inner sphere water molecule coordinated to the metal centre and/or the short local rotational correlation time (τ_{RL}) of the complex loaded on the nanoparticle. We have recently addressed the problem of the simultaneous optimization of k_{ex} and τ_{RL} using a GdDOTA-like complex (GdDOTA(GAC_{12})$_2$) functionalized with two hydrophobic chains on adjacent pendant arms that serve to rigidify the incorporated chelate.[20] The high relaxivity found in liposomes loaded with this complex was also confirmed *in vivo* at 1 T on a melanoma tumour model in mice.[21] Remarkably, the Gd-probe is rapidly cleared from the organs due to the presence of the two dodecyl chains. Although a rapid excretion of the agent is in many cases favourable, in other applications it is preferable that the complex remains embedded in the nanoparticle for longer times. This condition is typically achieved using amphiphiles containing two palmitoyl/stearyl chains.

[a] *Dipartimento di Biotecnologie Molecolari e Scienze della Salute, Centro di Imaging Molecolare e Preclinico, Università degli Studi di Torino, Via Nizza 52, Torino, 10126, Italia.*Corresponding author: E-mail: enzo.terreno@unito.it, Telephone: +39 011 6706452, Fax: +39 011 6706487.*
[b] *Dipartimento di Scienze ed Innovazione Tecnologica, Università del Piemonte Orientale "Amedeo Avogadro", Viale T. Michel 11, Alessandria, 15121, Italia.*Corresponding author: E-mail: lorenzo.tei@uniupo.it, Telephone: +39 0131 360 208, Fax: +39 0131 360250.*
Electronic Supplementary Information (ESI) available: details on the synthesis of GdDOTAGA(C_{18})$_2$ and physico-chemical characterization of paramagnetic nanoparticles. See DOI: 10.1039/x0xx00000x

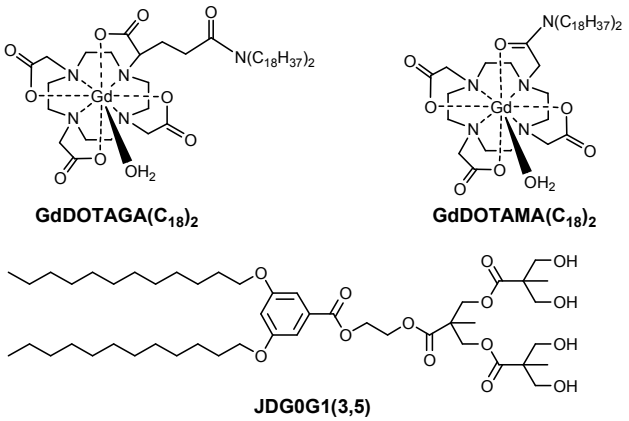

Scheme 1. Chemical structures of the amphiphilic Gd-chelates and of the Janus Dendrimer used for assembling dendrimersomes.

With the aim of combining the excellent incorporation stability of GdDOTAMA(C_{18})$_2$ into bilayered nanovesicles (liposomes, polymersomes, dendrimersomes)[7,22] with the high relaxivity offered by the tetra-carboxylic cage of GdDOTA(GAC_{12})$_2$, we synthesized the new amphiphilic chelate GdDOTAGA(C_{18})$_2$ (Scheme 1).

The motivation of this study was to investigate, either *in vitro* or *in vivo*, the imaging performance of nanovesicles (liposomes and dendrimersomes) loaded with GdDOTAGA(C_{18})$_2$, and make a comparison with the corresponding nanoparticles embedded with GdDOTAMA(C_{18})$_2$.

The synthesis of GdDOTAGA(C_{18})$_2$ was accomplished in four steps starting from DOTAGA(*t*Bu)$_4$ (Scheme S1): the free carboxylic acid was activated by formation of the *N*-hydroxysuccinimidyl ester, which was then reacted with dioctadecylamine in pyridine at 70°C. The free ligand was obtained after *t*Bu esters deprotection using a 1:1 mixture of TFA and dichloromethane and the Gd(III) complex was prepared by reacting the ligand with $GdCl_3$ in methanol at 50°C overnight. Liposomes and dendrimersomes (DSs) were prepared using the conventional film hydration method[7,23] (see ESI for details). DSs were formulated with the following moles percentage: 20% of the amphiphilic Gd-complex, 75% of a recently reported low generation Janus Dendrimer (JDG0G1(3,5), Scheme 1),[8] and 5% of DSPE-PEG2000-COOH. The pegylated phospholipid was used to improve particles stability and to confer stealthiness towards immune system.[7,8] Liposomes were formulated using the same composition, except for the presence of 75 % of DPPC instead of the dendrimer.

The magnetic field dependence of the relaxivity of the paramagnetic nanovesicles, the so-called nuclear magnetic relaxation dispersion (NMRD) profile, was measured at 25°C and 37°C, over the range 2.343×10^{-4}–1.645 T, which corresponds to proton Larmor frequencies varying from 0.01 to 70 MHz. The experimental profiles are reported in Figure 1 and S1 and show a peak centred around 30-40 MHz, which is characteristic of slowly tumbling systems.[14,15] A statistically higher relaxivity was measured for the nanovesicles (both liposomes and dendrimersomes) loaded with GdDOTAGA(C_{18})$_2$ with respect to the corresponding systems incorporating GdDOTAMA(C_{18})$_2$, whereas no relevant differences were observed between liposomes and dendrimersomes. The NMRD profiles were fitted using the conventional paramagnetic relaxation model (based on Solomon-Bloembergen-Morgan and Freed's theories)[14] implemented by the Lipari-Szabo approach,[24] which is used to describe the rotational dynamics when the (fast) rotation of the coordination cage of the complex (τ_{RL}) partially couples to the slow tumbling of the whole nanoparticle (τ_{RG}). Assuming that the τ_M value of the incorporated GdDOTAGA(C_{18})$_2$ is identical to that reported for the water soluble precursor GdDOTAGA,[20] the large

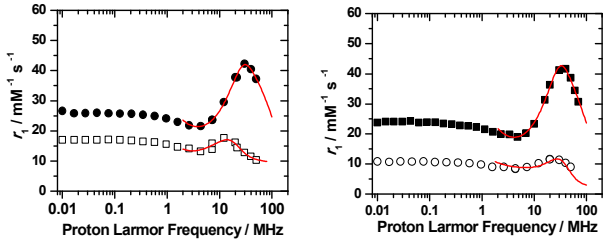

Figure 1. ^{1}H NMRD profiles at 298 K of paramagnetic dendrimerosomes (left) and liposomes (right) incorporating GdDOTAGA(C_{18})$_2$ (● and ■) and GdDOTAMA(C_{18})$_2$ (□ and ○).

Table 1. Relaxation parameters (at 25°C) obtained from the analysis of the NMRD profiles.[a,b]

Parameter	GdDOTAGA (C_{18})$_2$	GdDOTAMA (C_{18})$_2$	GdDOTAGA (C_{18})$_2$	GdDOTAMA (C_{18})$_2$
	liposome		dendrimersomes	
τ_M^{298} (ns)	130[c]	769[d]	130[c]	925[e]
τ_{RG}^{298} (ns)	80 ± 5	82	80 ± 5	80
τ_{RL}^{298} (ns)	1.96 ± 0.07	0.44	1.83 ± 0.05	0.55
S^2	0.43 ± 0.03	0.39	0.37 ± 0.04	0.65

[a] The parameters for electronic relaxation were used as empirical fitting parameters and have no real physical meaning for nanosized systems. Hence, the data at magnetic field < 3 MHz, which are the most affected by electronic relaxation, were not included in data analysis, in accordance with a well-established approach. For liposomes and dendrimersomes incorporating GdDOTAGA(C_{18})$_2$ Δ^2 has a value of (1.4 ± 0.1) and (1.1 ± 0.1)$\times10^{19}$ s^{-2} and τ_V of (14.3 ± 0.8) and (14.5 ± 0.2) ps, respectively. These values are comparable to those found for similar systems.[20,21] [b] The distance of the coordinated water molecule from the metal ion (r_{Gd-H}) was fixed to 3.0 Å. The outer-sphere component of the relaxivity was estimated by using standard values for the distance of closest approach, a (4 Å) and the relative diffusion coefficient of solute and solvent, D (2.24×10^{-5} cm^2 s^{-1}). [c] Ref. 20; [d] Ref. 21; [c] Ref. 7.

difference in the relaxivities of the two amphiphilic complexes in both nanovesicles can be mainly attributed to the different water exchange rates (Table 1). In fact, since the dioctadecyl moiety is connected similarly to both Gd-complexes, the τ_{RL} values and the order parameter S^2 (indicating the coupling between local and global motions) did not differ substantially for the two complexes, thus showing a similar degree of rotational flexibility. The r_1 values (30 MHz) of the complexes embedded in nanovesicles are shown in Figure 2. The plot highlights the remarkable relaxivity gain obtained by using GdDOTAGA(C_{18})$_2$. A similar r_1 value (40.0 mM^{-1} s^{-1}) was

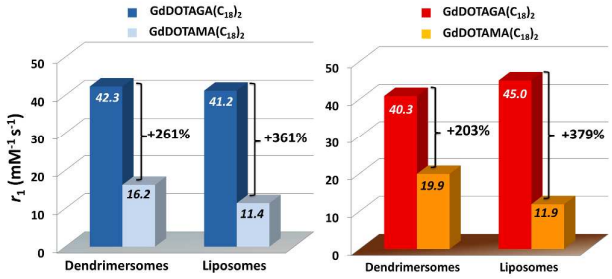

Figure 2. Relaxivity values of the paramagnetic nanovesicles at 30 MHz and 25 °C (left) and 37 °C (right) with highlighted the relaxivity gain obtained for the nanosystems incorporating GdDOTAGA(C_{18})$_2$.

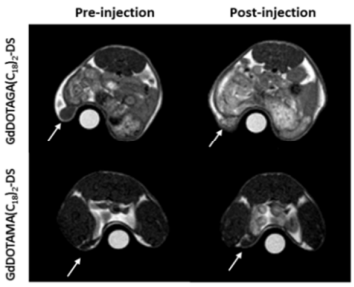

Figure 3. Representative axial T_{1w} images of the tumour (white arrows) immediately before or 10 min after the administration of GdDOTAGA(C_{18})$_2$ or GdDOTAMA(C_{18})$_2$-loaded dendrimersomes.

obtained for liposomes incorporating GdDOTA(GAC_{12})$_2$.[20,21] Noteworthy, the greatest change in relaxivity is observed for liposomes at 37°C where the enhancement of r_1 of GdDOTAGA(C_{18})$_2$ over the value observed for GdDOTAMA(C_{18})$_2$ is as large as +379%. The temperature dependence of r_1 is different for the two paramagnetic nanovesicles. By increasing temperature, the relaxivity of dendrimersomes slightly decreases for the vesicles embedding GdDOTAGA(C_{18})$_2$ and increases for those incorporating GdDOTAMA(C_{18})$_2$. This behaviour is a consequence of the different τ_M of the complexes that influences in a different manner the relaxivities. In the case of GdDOTAGA(C_{18})$_2$, r_1 is limited by the tumbling motion, thus by increasing the temperature the molecular rotation accelerates and r_1 decreases. On the other hand, for GdDOTAMA(C_{18})$_2$, r_1 is limited by k_{ex}, and the increase of the temperature is accompanied by an increase of r_1. However, in liposomes, a r_1 enhancement occurred also for GdDOTAGA(C_{18})$_2$. Likely, this observation reflects the lower water permeability of the liposome bilayer with respect to that of dendrimersomes.[7] Consequently, the contribution to the relaxivity arising from the complexes facing inward the liposomes cavity can be limited by the water diffusion across the membrane. Since this process is proportional to the temperature, the overall relaxivity at 37°C is higher than at 25°C.

Since no side effects of cytotoxicity (Figure S2) were observed on cells after the exposure to dendrimersomes incorporating Gd-DOTAGA(C_{18})$_2$ (referred to as GdDOTAGA(C_{18})$_2$-DS), the *in vivo* MRI performance of these nanoprobes was investigated on an experimental tumour model on a scanner operating at 1 T (40 MHz), and the results were compared to analogous dendrimersomes bearing the same percentage of Gd-DOTAMA(C_{18})$_2$ (GdDOTAMA(C_{18})$_2$-DS). Suspensions of the paramagnetic vesicles were systemically administered via tail vein to mice bearing subcutaneous syngeneic B16 melanoma (0.05 mmol Gd kg^{-1} body weight) and T_1-weighted images were acquired at different time points within two weeks to monitor the evolution of the T_1 Contrast Enhancement (T_1-CE) calculated as percentage in selected organs (liver, spleen, kidneys and tumour, Figure S3).

Within 2 hours after the injection, all the examined organs showed a general brightening for both the paramagnetic nanovesicles due to their circulation in blood (Figure 3, 4, S4 and S5). Nevertheless, the T_1-CE in all examined organs resulted to be significantly higher in animals receiving Gd-DOTAGA(C_{18})$_2$-DS. Several hours after the administration, the T_1-CE decreased in kidneys (both in renal cortex and pelvis), likely as a results of the clearance process and of the descending phase of the systemic circulation (Figure S4).

On the contrary, the T_1-CE in the organs devoted to the removal of the nanoparticles (*i.e.* liver and spleen) maintained stable for many days, preserving the difference initially calculated between the two cohorts of animals (Figure 4). Interestingly, after 24 h, the T_1-CE in liver increased with respect to the post-injection values, possibly reflecting the dynamics of the particle deposition in this tissue, which is controlled by the cellular effectors of the reticulo-endothelial system and may require a certain time to occur. Compared to the reference GdDOTAMA(C_{18})$_2$-DS, GdDOTAGA(C_{18})$_2$-DS showed a 2-3 fold increase in T_1-CE over the entire time window investigated. Gd^{3+} quantification by ICP-MS on the various explanted organs revealed an equivalent biodistribution pattern for the two employed nanosystems (Figure S6), thus confirming that the differences observed in the T_1-CE actually reflected the different contrast properties showed by the two amphiphilic complexes.

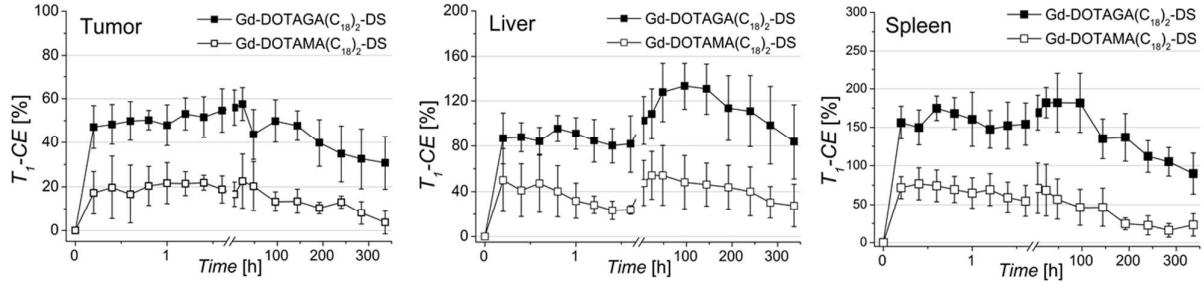

Figure 4. Time evolution of the percentage T_1 Contrast Enhancement (T_1-CE) calculated on T_1-weighted images of tumor, liver and spleen of mice systemically injected with GdDOTAGA(C_{18})$_2$ or GdDOTAMA(C_{18})$_2$-loaded dendrimersomes (black squares and white squares, respectively).

However, both imaging and biodistribution profiles indicate a long-term *in vivo* retention of the nanoprobes, which could possibly entail some safety risks in real biological use.

In conclusion, we have reported the first *in vivo* MRI application of paramagnetic dendrimersomes incorporating a new, highly efficient, amphiphilic Gd-complex. The several favourable properties of this GdDOTA-like chelate, namely the high thermodynamic stability and kinetic inertness provided by the DOTA cage, the fast k_{ex}, the fairly easy preparation, and the improved relaxivity of the resulting lipid nanoparticles embedding the chelate, are expected to favour its widespread use in MRI and theranostic applications. We also confirmed that dendrimersomes might represent a valuable alternative to the use of liposomes, and can be appealing agents for the development of improved *in vivo* diagnostic and theranostic protocols.

The financial support of the "Compagnia di San Paolo" (CSP-2012 NANOPROGLY and ''Validazione di molecole di tipo VHH e Aptameri per il rilascio tumore-specifico di farmaci e la valutazione contestuale della risposta mediante imaging funzionale mirato'' projects), University of Torino (Innovative Nanosized Theranostic Agents) and European Union's FP7/2007–2013 under grant agreement no. HEALTH-F2-2011-278850 (INMiND) is gratefully acknowledged. This work was carried out within the framework of the COST TD1004 Action.

Notes and references

1 M.G. De Morais, V.G. Martins, D. Steffens, P. Pranke, J.A. da Costa, *J. Nanosci. Nanotech.,* 2014*,* **14**, 1007.
2 M. S. Muthu, D. T. Leong, L. Mei and S. S. Feng, *Theranostics*, 2014, **4**, 660.
3 J.H. Ryu, S. Lee, S. Son, S.H. Kim, J.F. Leary, K. Choi, I.C. Kwon, *J. Control. Release*, 2014, **190**, 477.
4 S.Nazir, T. Hussain, A. Ayub, U. Rashid and A. J. MacRobert, *Nanomedicine*, 2014, **10**, 19.
5 W. Mehnert and K. Mäder, *Adv. Drug Deliv. Rev.*, 2001, **47**, 165.
6 V. Percec, D. A. Wilson, P. Leowanawat, C. J. Wilson, A. D. Hughes, M. S. Kaucher, D. A. Hammer, D. H. Levine, A. J. Kim, F. S. Bates, K. P. Davis, T. P. Lodge, M. L. Klein, R. H. DeVane, E. Aqad, B. M. Rosen, A. O. Argintaru, M. J. Sienkowska, K. Rissanen, S. Nummelin, J. Ropponen, *Science,* 2010, **328**, 1009.
7 M. Filippi, J. Martinelli, G. Mulas, M. Ferraretto, E. Teirlinck, M. Botta and E. Terreno, *Chem. Commun.,* 2014, **50**, 3453.
8 M. Filippi, D. Patrucco, J. Martinelli, M. Botta, P. Castro-Hartmann , L. Tei and E. Terreno, *Nanoscale*, 2015, **7**, 12943.
9 M. Uner and G. Yener, *Int. J. Nanomedicine*, 2007, **2**, 289.
10 H.I. Chang and M.K. Yeh, *Int. J. Nanomedicine*, 2012, **7**, 49.
11 W.T. Al-Jamal and K. Kostarelos, *Acc. Chem. Res.*, 2011, **44**, 1094.
12 D.A. Groneberg, M. Giersig, T. Welte and U. Pison, *Curr. Drug Targets*, 2006, **7**, 643.
13 G. A. Rolla, M. Botta, L. Tei, C. Cabella, S. Ghiani, C. Brioschi, A. Maiocchi, *Chem. Eur. J.*, 2013, **19**, 11189.
14 S. Aime, M. Botta, E. Terreno, *Adv. Inorg. Chem.,* 2005, **57**, 173.
15 M. Botta, L. Tei, *Eur. J. Inorg. Chem.*, 2012, **12**, 1945.
16 a) A. Accardo, D. Tesauro, A. Luigi, C. Pedone and G. Morelli, *Coord. Chem. Rev.*, 2009, **253**, 2193. b) W. J. M. Mulder, G. J. Strijkers, G. A. F. Van Tilborg, A. W. Griffioen and K. Nicolay, *NMR. Biomed.*, 2006, **19**, 142. c) E. Terreno, D. Delli Castelli, C. Cabella, W. Dastrù, A. Sanino, J. Stancanello, L. Tei and S. Aime, *Chem. Biodivers.*, 2008, **5**, 1901.
17 I. Bertini, F. Bianchini, L. Calorici, S. Colagrande, M. Fragai, A. Franchi, O. Gallo, C. Gavazzi and C. Luchinat, *Magn. Reson. Med.*, 2004, **52**, 669.
18 P. L. Anelli, L. Lattuada, V. Lorusso, M. Schneider, H. Tournier and F. Uggeri, *MAGMA*, 2001, **12**, 114.
19 a) S. Hak, H.M.H.F. Sanders, P. Agrawal, S. Langereis, H. Grüll, H.M. Keizer, F. Arena, E. Terreno, G.J. Strijkers, K. Nicolay, *Eur. J. Pharm. Biopharm.*, 2009, **72**, 397; b) S. Langereis, T. Geelen, H. Grüll, G. J. Strijkers and K. Nicolay, *NMR. Biomed.*, 2013, **26**, 72.
20 F. Kielar, L. Tei, E. Terreno, M. Botta, *J. Am. Chem. Soc.*, 2010, **132**, 7836.
21 E. Cittadino, M. Botta, L.Tei, F. Kielar, R. Stefania, E. Chiavazza, S. Aime and E. Terreno, *Chempluschem.*, 2013, **78**, 712.
22 a) C. Grange, S. Geninatti Crich, G. Esposito, D. Alberti, L. Tei, B. Bussolati, S. Aime, and G. Camussi, *Cancer Res.*, 2010, **70**, 2180; b) H. Grüll, S. Langereis, L. Messager, D. Delli Castelli, A. Sanino, E. Torres, E. Terreno, S. Aime, *Soft Matter*, 2010, **6**, 4847.
23 M.R. Mozafari, *Cell. Mol. Biol. Lett.,* 2005, **10**, 711.
24 a) G. Lipari and S. Szabo, *J. Am. Chem. Soc.*, 1982, **104**, 4546; b)G. Lipari and S. Szabo, *J. Am. Chem. Soc.,* 1982, **104**, 4559.